

Accuracy of a cone beam computed tomography–guided surgical stent for orthodontic mini-implant placement

Jae-Jung Yu^a; Gyu-Tae Kim^b; Yong-Suk Choi^c; Eui-Hwan Hwang^d; Janghyun Paek^e; Seong-Hun Kim^f; John C. Huang^g

ABSTRACT

Objective: To validate the accuracy of a cone-beam computed tomography (CBCT)–guided surgical stent for orthodontic mini-implant (OMI) placement by quantitatively evaluating the difference between CBCT-prescribed and actual position of mini-implants in preoperative and postoperative CBCT images.

Materials and Methods: A surgical stent was fabricated using Teflon-Perfluoroalkoxy, which has appropriate biological x-ray attenuation properties. Polyvinylsiloxane impression material was used to secure the custom-made surgical stent onto swine mandibles. CBCT scanning was done with the stent in place to virtually plan mini-implants using a three-dimensional (3D) software program. An appropriate insertion point was determined using 3D reconstruction data, and the vertical and horizontal angulations were determined using four prescribed angles. A custom-designed surveyor was used to drill a guide hole within the surgical stent as prescribed on the CBCT images for insertion of 32 OMIs. The mandibles with a surgical stent in place were rescanned with CBCT to measure the deviations between the virtual planning data and surgical results.

Results: The difference between the prescribed and actual vertical angle was 1.01 ± 7.25 , and the horizontal difference was 1.16 ± 6.08 . The correlation coefficient confirms that there was no intrarater variability in either the horizontal ($R = .97$) or vertical ($R = .74$) vectors.

Conclusions: The surgical stent in this study guides mini-implants to the prescribed position as planned in CBCT. Since the statistical difference was not significant, the surgical stent can be considered to be an accurate guide tool for mini-implant placement in clinical use. (*Angle Orthod.* 2012;82:275–283.)

KEY WORDS: Mini-implant; Root proximity; Surgical stent; CBCT

^a Instructor, Department of Oral and Maxillofacial Radiology, Kangdong Sacred Heart Hospital, Hallym University Medical Center, Seoul, Korea.

^b Full-time Lecturer, Department of Oral and Maxillofacial Radiology, Kyung Hee University, Seoul, Korea.

^c Associate Professor and Department Chair, Department of Oral and Maxillofacial Radiology, Kyung Hee University, Seoul, Korea.

^d Professor, Department of Oral and Maxillofacial Radiology, Kyung Hee University, Seoul, Korea.

^e Clinical Fellow, Department of Prosthodontics, Kyung Hee University, Seoul, Korea.

^f Associate Professor, Department of Orthodontics, College of Dentistry, Kyung Hee University, Seoul, Korea.

^g Associate Clinical Professor and Vice Chair, Division of Orthodontics, Department of Orofacial Science, University of California, San Francisco.

Corresponding author: Dr Seong-Hun Kim, Department of Orthodontics, College of Dentistry, Kyung Hee University, #1 Hoegi-dong, Dongdaemun-gu, Seoul 130-701, Republic of Korea (e-mail: bravortho@hanmail.net and bravortho@khu.ac.kr)

Accepted: July 2011. Submitted: June 2011.

Published Online: August 29, 2011

© 2012 by The EH Angle Education and Research Foundation, Inc.

INTRODUCTION

Immediate-load orthodontic mini-implants (OMIs) for intraoral orthodontic anchorage are reliable anchorage mechanisms to achieve the desired amount of tooth movement without patient compliance.^{1,2} To achieve an effective result, the stability at the initial stage is very important. Therefore, precise placement in the interradicular space is critical because root proximity has been defined to be a major risk factor of initial stability.³

A number of studies have attempted to survey optimal locations for mini-implant placement.^{4–8} Several methods use periapical radiography, panoramic radiography, computed tomography, and cone-beam computed tomography (CBCT).^{3–5,9} However, conventional periapical and panoramic imaging techniques combined with visual inspection are insufficient to obtain accurate presurgical planning¹⁰ because of inherent distortions of the radiographic images. CT is isotropically accurate but has been limited in dentistry due to its high cost, lower image resolution, and high radiation dose.¹¹

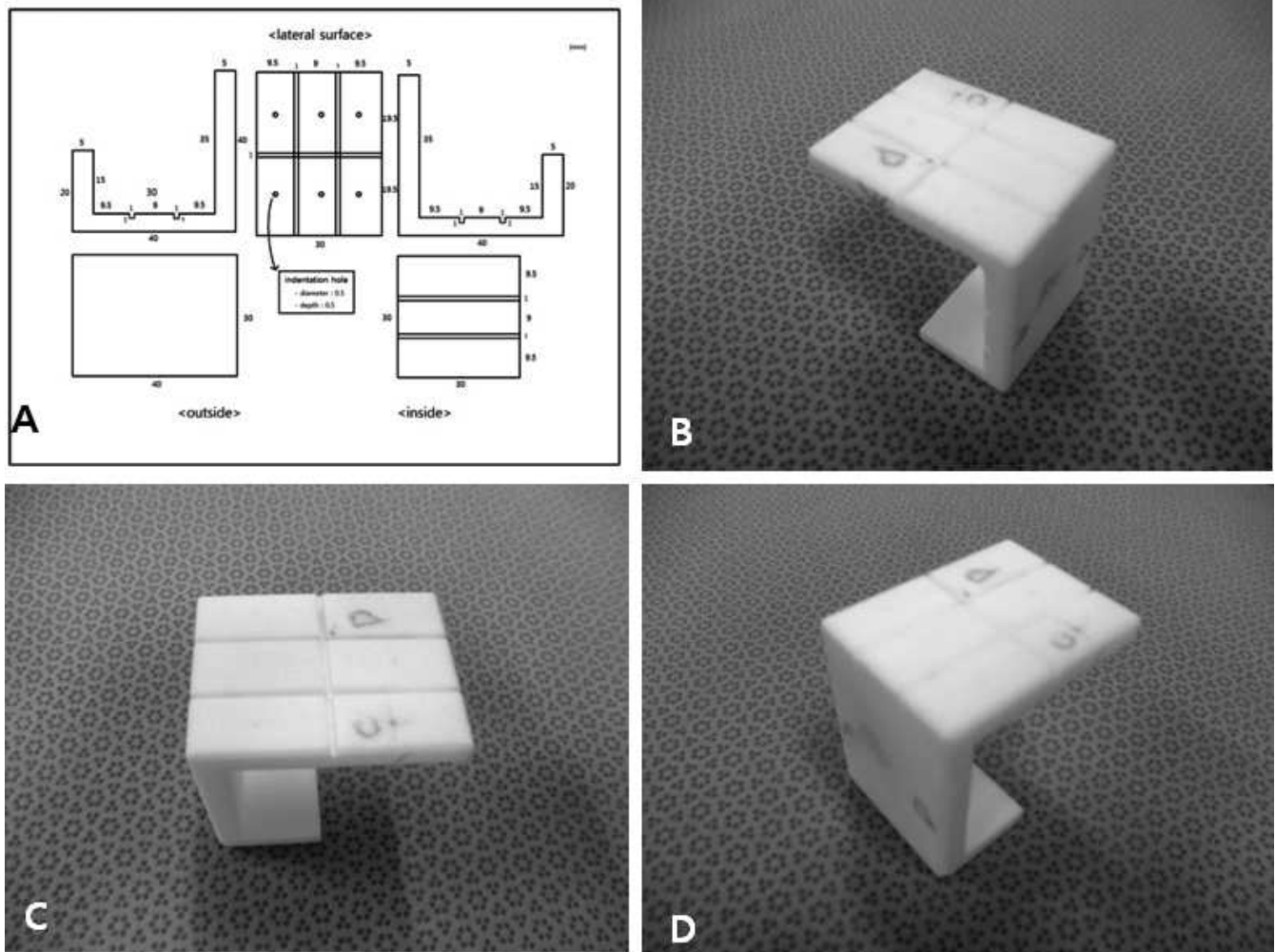


Figure 1. (A) Template for newly developed cone-beam computed tomography–assisted surgical stent for orthodontic mini-implant placement (numerical values are linear measurements in millimeters). (B–D) Actual surgical guide stent.

The recently developed CBCT has overcome many of the limitations of conventional dental radiographic techniques by providing reasonable tissue contrast, minimizing blurring and overlapping of adjacent teeth, and offering orthogonal views by eliminating projection artifacts. Additional advantages of CBCT include reduced cost and significant reduction of radiation exposure compared with typical medical CT devices.¹²

The clinical application of CBCT in fabricating an OMI surgical stent allows for more accurate and safe placement of OMIs in the interradicular spaces of the alveolar area. Therefore, several surgical guide systems have been developed to obtain safer mini-implant insertion between teeth roots, avoiding accidents and complications. One method used to obtain an accurate surgical guide is stereolithography, but this procedure requires elaborate technology, great complexity, and high cost.^{5,13,14} Other surgical guides can be hand-made, but stent accuracy is directly dependent on presurgical radiographic standardization to avoid

oblique projections and distorted radiographic images, which will lead to mistaken interpretations about a putative safe insertion site.^{3,4,7}

Choi et al.¹⁵ developed a new navigation guide for addressing limitations of existing CBCT guide systems. Using this technique, a surgical stent is custom made from rubber polyvinylsiloxane (PVS) impression material, and the rubber stent and jaw are scanned together using CBCT. The production process is a mathematically calculated process that does not require intermediate steps or additional model making; this geometric algorithm leads to a definitive decision for optimal OMI placement site. Statistically significant differences were not observed between the predictive implant location and actual implant location.

The aim of the present in vitro study was to quantify the accuracy of a system for a CBCT-guided surgical stent for OMI insertion by evaluating the difference between prescribed and actual mini-implant positions



Figure 2. Dental impression was taken using polyvinylsiloxane and trimmed to fit the shape of the surgical stent.

on preoperative and postoperative CBCT scans using swine mandibles.

MATERIALS AND METHODS

This study did not require approval by the university’s Institutional Review Board, and no patients were involved in this research. This study used four

mandibles from swine that were killed at approximately 3 months of age. A surgical stent was fabricated using Teflon-Perfluoroalkoxy (PFA) with an appropriate x-ray attenuation and easy handling.¹⁴ The lateral surface of the surgical stent has six equally divided parts with an indentation hole marking each center (Figure 1). These indentation holes will be used as geometric landmarks for referencing on the CBCT data set, and conversely it will also be used for transposing spatial information obtained from CBCT imaging to the surgical stent surface. The surgical stent-mandible complex secured using PVS impression material was scanned using an Alphard-3030 CBCT scanner (Asahi Roentgen Ind. Co, Kyoto, Japan), and data were saved in DICOM (digital imaging and communications in medicine) format using the Picture Archiving Communication System (Infinit, Seoul, Korea) at Kyung Hee Dental Hospital (Figure 2). The appropriate OMI insertion point was determined by analyzing multiplanar reconstruction images and three-dimensional (3D) reconstruction data using the OnDemand 3D software program (CyberMed, Seoul, Korea); from this insertion point, the distances to the nearest three adjacent indentation holes were measured (Figure 3). The horizontal OMI insertion point of the bone surface was determined in the middle of the interradicular space or between the mesial and distal root, and the vertical point was the center of the root length. This information is transferred directly to the flat lateral surface of the physical Teflon-PFA surgical guide template by using

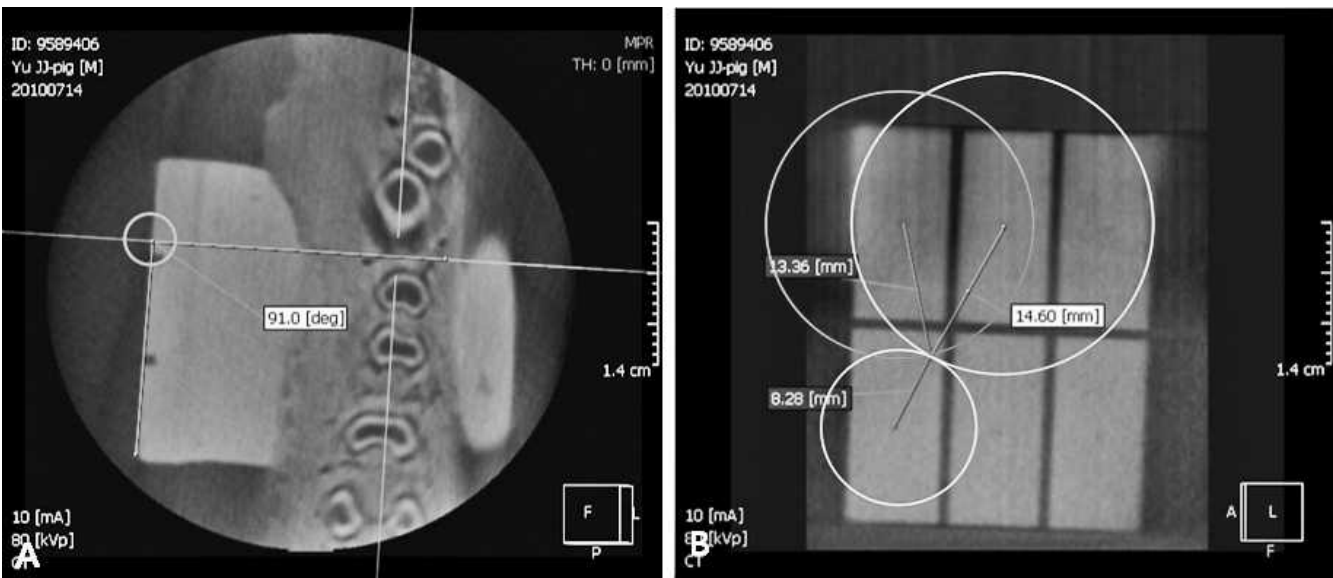


Figure 3. (A) The insertion point position for proper orthodontic mini-implant implantation was identified using image slices from cone-beam computed tomography data. (B) On the lateral flat surface of the surgical stent template, linear distances were measured from the insertion point to the three closest indentation holes. This information can be transferred to the physical Teflon-Perfluoroalkoxy surgical guide template by drawing the same circles on the stent using the correlative indentation holes as centers. The intersection of all three circles effectively reproduces the insertion point identified on the computer.

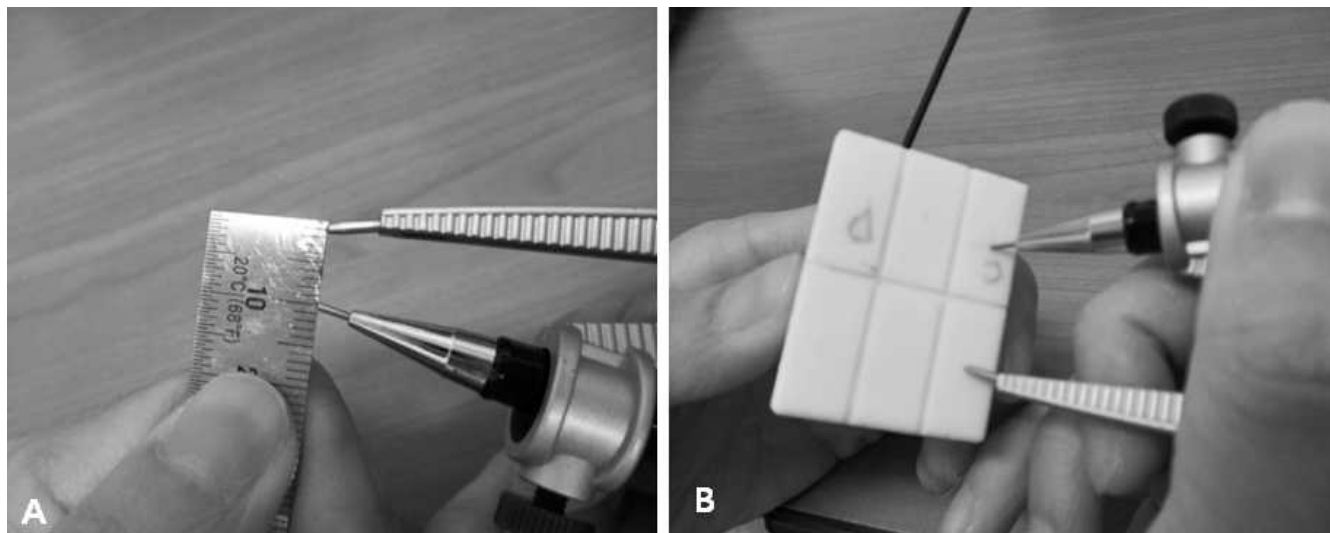


Figure 4. (A) The length of each line was calibrated to a drawing compass. (B) Circular arcs were drawn directly on the surgical guide with each indentation hole as the center. The junction of all three circles created one intersection that reproduces the insertion point for the guide hole specified on the cone-beam computed tomography image.

a compass to draw the same circles on the stent using the correlative indentation holes as centers (Figure 4). The intersection of all three circles effectively reproduces the insertion point that was identified on the computer.

The vertical angulations to the long axis of adjacent teeth were determined at four prescribed angles (30°, 45°, 60°, and 75°). The prescribed vertical and horizontal angulations for the surgical stent surface were measured at each angle (Figure 5), and the data were used to decide the bucco-lingual inclination angle and mesio-distal inclination angle. This information

was transferred to an aluminum custom-designed surveyor for drilling of the guide hole on the surgical stent. The 2.7-mm-diameter guide hole was designed to minimize any insertion error during OMI placement (Figure 6).

A total of 32 OMIs (screw diameter for bone penetration = 1.8 mm; largest diameter = 2.5 mm; length = 8.5 mm; C-implant, Cimplant Co, Seoul, Korea) were placed into the bone using a CBCT-guided surgical stent with manual drilling (Figure 7). The postoperative swine mandible with surgical stent was rescanned with CBCT to measure the deviations

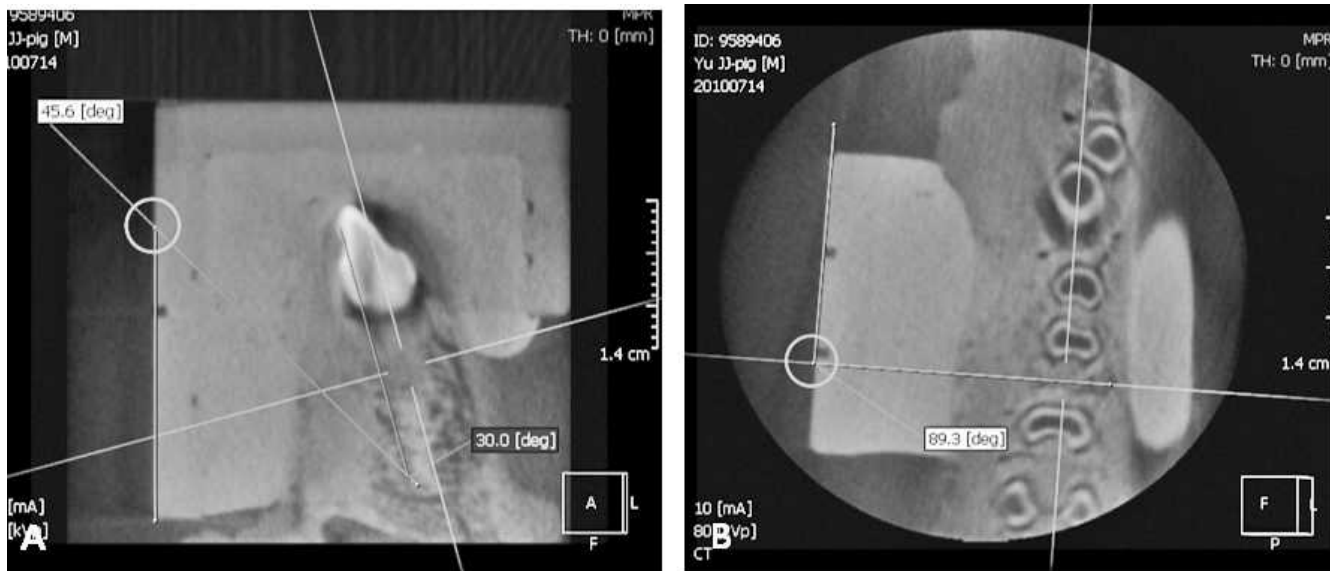


Figure 5. (A) Measurement of the vertical insertion angle to the stent surface (30°, 45°, 60°, and 75° to the long axis of adjacent tooth). (B) Measurement of the horizontal insertion angle to the stent surface (avoiding root). From this insertion point, the bucco-lingual inclination angle and the mesio-distal inclination angle were decided, and the prescription was transferred to the surgical stent template.

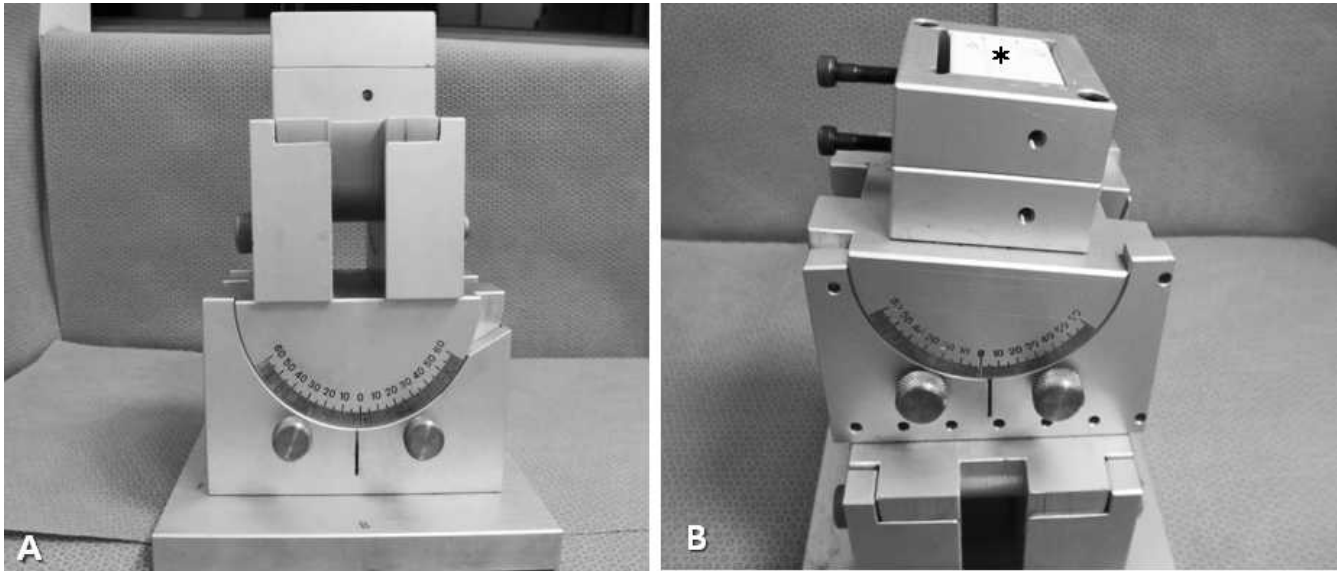


Figure 6. (A) Custom-designed and custom-manufactured surveyor system with rotational ability in all three planes. (B) Surgical stent (*) placed in the surveyor system. By using the custom-designed surveyor and a CNC machine, a guide hole was drilled in the surgical stent template according to the prescription angles measured on the cone-beam computed tomography data.

between the virtual planning data and actual surgical outcomes (Figure 8). The same examiner measured the postoperative angulations after 2 weeks to confirm intrarater reliability.

Statistical Analysis

The means and standard deviations of the measurements were calculated using SAS 9.1 software (SAS Korea, Seoul, Korea). A correlation analysis was performed for initial data and recalibrating data. The mean value obtained from prescribed angles versus actual angles was compared using the Student's *t*-test ($P < .05$) to assess the reproducibility of the surgical

stent, and the mean value differences for each group were evaluated.

RESULTS

Examining the statistical analysis of measurement error, the correlation coefficient between initial data and recalibrating data is .97 in vertical angulation and .74 in horizontal angulation (Table 1). Raw data results of vertical angulation are presented in Table 2. The difference between the prescribed vertical and actual vertical angulation showed that for the total group mean, the prescribed angle was 93.06° compared with an actual mean angle of 94.08° (Table 3). The $P =$

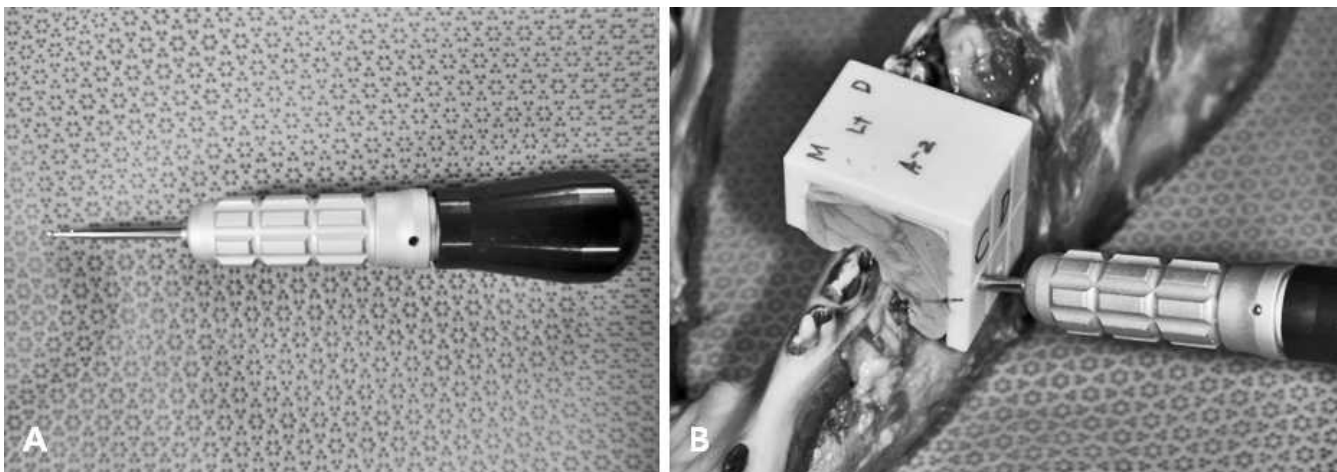


Figure 7. (A) A 1.5-mm-diameter hand drill (drill nose diameter = 2.5 mm). The drill nose diameter is the same as the orthodontic mini-implant (OMI) driver tip. (B) Cone-beam computed tomography-guided surgical stent used to insert a 1.5-mm OMI with a hand drill.

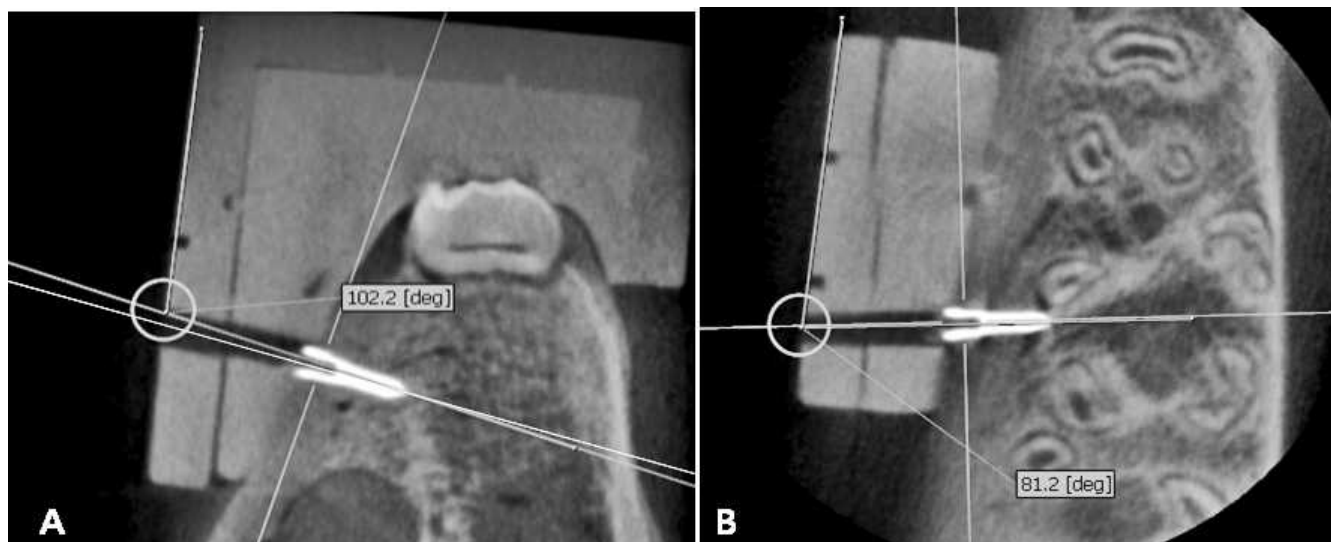


Figure 8. After implantation of the mini-implant, the angle between the long axis of the mini-implant (A) and stent surface (B) was measured to evaluate the reproducibility of the surgical stent. White line indicates planned insertion direction.

.908 value validates that there was no statistically significant difference between prescribed versus actual angulation. All measured values for evaluating the horizontal angulation are presented (Table 4). Focusing on the variation between the prescribed horizontal versus actual horizontal angulation, for the total group the prescribed mean angle was 90.25° , and the actual mean angle measured 91.41° ($P = .388$), so there was no statistically significant difference between the two data sets (Table 5).

DISCUSSION

Criteria for defining the success of OMI use are as follows: absence of inflammation, absence of clinically detectable mobility, and capability of sustaining the anchorage function as needed throughout the course of orthodontic treatment.¹⁶ A common complication is clinical failure of the mini-implant. Surface-treated OMIs have been introduced as firm anchorage systems that can achieve partial osseointegration during treatment.^{3,17} Many factors have been linked to initial stability of OMIs, including insertion mechanism, thread design, proximity to adjacent root/periodontal structures, OMI length, and OMI angulation.

Table 1. Measurement of Error Between First and Second Time Interval^a

	Mean	SD	R	P Value
Vertical	93.34	38.35	.96635	<.0001
Re-vertical	91.14	38.95		
Horizontal	91.68	6.27	.74212	<.0001
Re-horizontal	90.57	5.88		

^a SD indicates standard deviation; R, correlation coefficient.

Kuroda et al.¹⁸ published research using two-dimensional analysis showing that root proximity was identified as a major risk factor of initial stability for OMIs. However, they used mainly periapical images as their diagnostic aids, which have inherent image distortions depending on x-ray tube angulation. Some CT studies have measured interradiacal space for OMIs to assess postsurgical position.^{9,19,20} Liou et al.²¹ recommend 2 mm of safety clearance between OMI and the dental root; thus, a 1.5-mm-diameter OMI would require 5.5 mm of interradiacal septal width to ensure root integrity, making OMI placement impossible in most sites. Contrary to these previous studies, the research on removal torque value by Kim et al.²² showed that the surface-treated OMI surface can provide stationary anchorage within a narrow interradiacal space. Kim et al.,³ using 3D CBCT to evaluate root proximity of installed C-implants, indicated that root proximity by itself was not a major risk factor for OMI failure but may lead to loss of primary stability and subsequent loosening of the OMI.

Deguchi et al.²³ suggested that angulation of OMI placement increases retention and recommended an angle of approximately 30° to the long axis of the tooth to increase the bone interdigitation of these miniscrews. At an oblique angle, the OMI can attain a longer distance through cortical bone and achieve higher initial stability. However, Byoun et al.²⁴ suggested that the successful placement of the OMI is more closely related to the diameter and contact point of the mini-implant into the cortical bone surface rather than the insertion angle.

Safety is a major consideration for OMI placement in the bone and can be achieved by ensuring that the

Table 2. Summarized Results of Measured Vertical Angulation

30°		45°		60°		75°	
Prescribed Angle, °	Actual Angle, °	Prescribed Angle, °	Actual Angle, °	Prescribed Angle, °	Actual Angle, °	Prescribed Angle, °	Actual Angle, °
44.8	46.1	118.2	124.3	104.1	95.7	86.1	83.7
38.8	35.8	52.5	50.7	111.2	106.4	96.5	92.9
45.6	41.0	126.4	128.8	113.2	107.3	91.5	97.1
34.4	30.3	48.8	39.2	113.2	107.2	96.7	94.4
38.3	46.1	43.9	41.3	108.6	107.3	93.2	102.2
140.4	144.2	49.8	63.8	119.2	114.4	104.6	132.0
137.7	137.8	122.8	122.8	109.5	110.4	95.9	99.1
145.2	154.0	130.4	130.1	116.7	122.2	99.7	101.8

proposed OMI site has adequate interradicular space to accommodate the diameter of the mini-implant, thereby avoiding any root damage. Complications during OMI insertion can range from slight root contact causing screw failure to extreme severe root perforation causing pulp damage or tooth loss. Most orthodontists generally place mini-implants without a surgical guide and take only a panoramic radiograph or periapical images for presurgical treatment planning to estimate interradicular space.^{3,4,7} When implant installation is done manually without a surgical guide, the implant tends to follow the trajectory of least resistance.¹⁰

In this study, CBCT was used to fabricate a surgical stent guide for OMI insertion and then subsequently used to compare the virtual prescribed OMI position relative to the actual OMI installation surgical outcome using the stent. The angular deviations between virtual and actual implant placement in both horizontal and vertical planes were compared using the CBCT data sets. The calculated *p* values of the statistical analyses confirmed the null hypothesis stating that there is no difference between virtual and actual surgical OMI positions.

The direct transfer of preoperative planning data to the actual site is extremely complex and difficult. In conventional surgical guide methods, the ideal implantation site is assumed on the gypsum model, which is uniform with the patient’s dentition. The success of this method relies highly on the operator’s experience. Jabero and Sarment²⁵ referred to this error as the “missing link.” To overcome this error, more accurate surgical guides and methods such as stereolithographic surgical stent, computer-aided design and

computer-aided manufacturing, a real-time surgical navigation system, and other tools have been introduced to clinicians, but these protocols require high cost and considerable time. Miyazawa et al.²⁶ used surgical guides fabricated from dental casts to place OMIs. During the process of altering the site and angulation of the guide tube using CBCT imaging, errors are inevitable because of the lack of correlation between the information from the imaging system onto the guide. Thus, a combination of diagnostic guide and surgical stent with indentation holes directing the mini-implant to the prescribed position was invented in this study.

After CBCT scan, the decision-making process for prescription of mini-implant location using information drawn from multiplanar reconstruction images was performed with the following sequence: (1) determine the insertion site, (2) measure the distance from the insertion site to the adjacent three indentation holes for guide hole formation and subsequent determination of guide hole direction, and (3) define the diameter and depth of mini-implant. The mesio-distal angle and bucco-lingual angles were measured at the insertion point, and the data were transferred onto the surgical stent. A distinct advantage of this method over a conventional surgical guide is the direct transposition of geometric data from the computer to the surgical stent. From this study, an accurate guide hole can be formed using a newly developed surveyor that transfers prescription angle from CBCT scan to surgical stent. Thus, this study provided a new application of the conventional CBCT-based navigation guide for the OMI.

Table 3. Comparison Between Prescribed and Actual Measurement of the Vertical Insertion Angle

Group	Prescribed Angle		Difference (Mean ± SD)	Actual Angle		P Value
	Mean	SD		Mean	SD	
Total (N = 32)	93.06	34.13	1.01 ± 7.25	94.08	35.74	.908
30° (n = 8)	78.15	52.28	1.26 ± 5.19	79.41	55.0	.963
45° (n = 8)	86.6	40.67	1.02 ± 6.89	87.63	42.26	.961
60° (n = 8)	111.96	4.75	-3.1 ± 4.51	108.86	7.54	.342
75° (n = 8)	95.52	5.51	4.8 ± 10.08	100.4	14.07	.385

Table 4. Summarized Results of Measured Horizontal Angulation

30°		45°		60°		75°	
Prescribed Angle, °	Actual Angle, °	Prescribed Angle, °	Actual Angle, °	Prescribed Angle, °	Actual Angle, °	Prescribed Angle, °	Actual Angle, °
100.4	94.0	94.6	100.0	88.6	85.8	84.3	87.9
90.56	96.1	89.2	90.8	89.6	96.2	84.9	93.4
89.3	85.8	94.6	98.7	84.7	97.7	91.0	94.8
88.9	88.4	84.4	81.5	100.7	94.7	84.6	90.1
93.1	90.2	92.5	93.4	94.1	100.6	96.1	98.8
85.8	98.9	88.5	88.8	94.6	93.6	95.5	81.3
88.6	100.4	84.8	88.0	91.5	89.9	83.9	80.4
89.5	89.0	86.6	85.7	90.7	85.7	91.8	86.2

Table 5. Comparison Between Prescribed and Actual Measurement of the Horizontal Insertion Angle

Group	Prescribed Angle		Difference (Mean ± SD)	Actual Angle		P Value
	Mean	SD		Mean	SD	
Total (N = 32)	90.25	4.55	1.16 ± 6.08	91.41	5.91	.383
30° (n = 8)	90.77	4.38	2.08 ± 7.26	92.85	5.30	.407
45° (n = 8)	89.40	4.12	1.24 ± 3.00	90.64	6.54	.658
60° (n = 8)	91.81	4.77	1.21 ± 6.71	93.02	5.45	.643
75° (n = 8)	89.01	5.19	0.1 ± 7.39	89.11	6.46	.973

For this CBCT-assisted OMI stent fabrication process, some potential sources of error include data from the CBCT scan (eg, patient movement causing blurriness of images), transposing the guide hole planning data, manufacturing of the surgical stent, positioning of the surgical stent, and during installation of the OMI (Figure 8A). However, as shown by the data of this study, if all parameters are well controlled, one can achieve ideal results. The stability of the surgical stent is a critical factor. In this study, the surgical stent was supported by three surfaces consisting of teeth, lingual mucosa, and buccal mucosa. Another consideration is that the swine bone is slightly harder than live human bone, especially when compared with cortical bone of the human mandible and theoretically may possibly deflect the drills to a minor degree compared with in vivo on a real patient, but the clinical outcomes differences would likely be negligible.

CONCLUSIONS

- Using the CBCT scan for identifying suitable mini-implant sites and its subsequent application in the fabrication of a stent guide can optimize both the clinical success and safety rates of OMI treatment.
- For postoperative stability, the use of a surgical stent is highly recommended to minimize the risk of incurring root contact with the mini-implant.

ACKNOWLEDGMENT

This study is based on a research thesis completed at the Kyung Hee University.

REFERENCES

1. Chen YJ, Chang HH, Lin HY, Lai E, Hung HC, Yao CC. Stability of miniplates and miniscrews used for orthodontic anchorage: experience with 492 temporary anchorage devices. *Clin Oral Implant Res.* 2008;19:1188–1196.
2. Antoszewska J, Trześniewska P, Kawala B, Ludwig B, Park HS. Qualitative and quantitative evaluation of root injury risk potentially burdening insertion of miniscrew implants. *Korean J Orthod.* 2011;41:112–120.
3. Kim SH, Kang SM, Choi YS, Kook YA, Chung KR, Huang JC. Cone-beam computed tomography evaluation of mini-implants after placement: is root proximity a major risk factor for failure? *Am J Orthod Dentofac Orthop.* 2010;138:264–276.
4. Estelita S, Janson G, Chiqueto K, Janson M, Freitas M. Predictable drill-free screw positioning with a graduated 3-dimensional radiographic-surgical guide: a preliminary report. *Am J Orthod Dentofacial Orthop.* 2006;136:722–735.
5. Kim SH, Choi YS, Hwang EH, Chung KR, Kook YA, Nelson G. Surgical positioning of orthodontic mini-implants with guides fabricated on models replicated with cone-beam computed tomography. *Am J Orthod Dentofacial Orthop.* 2007;131(suppl):S82–S89.
6. Kitai N, Yasuda Y, Takada K. A stent fabricated on a selectively colored stereolithographic model for placement of orthodontic mini-implants. *Int J Adult Orthod Orthognath Surg.* 2002;17:264–266.
7. Baros S, Janson G, Chiqueto K, Garib D. Two-dimensional radiographic and clinical references of the tooth crown for orthodontic mini-implant insertion: a guide-free technique. *Oral Surg Oral Med Oral Pathol Oral Radiol Endod.* 2010;110:e8–e16.
8. xLiu H, Liu D-X, Wang G, Wang CL, Zhao Z. Accuracy of surgical positioning of orthodontic miniscrews with a computer-aided design and manufacturing template. *Am J Orthod Dentofacial Orthop.* 2010;137:728.e1–728.e10.
9. Poggio PM, Incorvati C, Velo S, Carano A. “Safe zones”: a guide for miniscrew positioning in the maxillary and mandibular arch. *Angle Orthod.* 2006;76:191–197.

10. D'haese J, Van De Velde T, Komiyama A, Hultin M, De Bruyn H. Accuracy and complications using computer-designed stereolithographic surgical guides for oral rehabilitation by means of dental implants: a review of the literature. *Clin Implant Dent Relat Res*. In press.
11. Saliva M, Wolf U, Heinicke F, Bumann A, Visser H, Hirsch E. Cone-beam computed tomography for routine orthodontic treatment planning: a radiation dose evaluation. *Am J Orthod Dentofacial Orthop*. 2008;133:640.e1–640.e5.
12. Kwong J, Paloma J, Landers M, Figueroa A, Hans M. Image quality produced by different cone-beam computed tomography settings. *Am J Orthod Dentofacial Orthop*. 2008;133:317–327.
13. Son KH, Park JW, Lee DK, Kim KD, Baek SH. New virtual orthodontic treatment system for indirect bonding using the stereolithographic technique. *Korean J Orthod*. 2011;41:138–145.
14. Kim SH, Kang JM, Choi B, Nelson G. Clinical application of a stereolithographic surgical guide for simple positioning of orthodontic mini-implants. *World J Orthod*. 2008;9:371–382.
15. Choi HS, Kim GT, Choi YS, Hwang EH. Surgical stent for dental implant using cone beam CT images. *Korean J Oral Maxillofac Radiol*. 2010;40:171–178.
16. Wiechmann D, Meyer U, Büchter A. Success rate of mini- and micro-implants used for orthodontic anchorage: a prospective clinical study. *Clin Oral Implants Res*. 2007;18:263–267.
17. Park SH, Kim SH, Ryu JH, Kang YG, Chung KR, Kook YA. Bone-implant contact and mobility of surface-treated orthodontic micro-implants in dogs. *Korean J Orthod*. 2008;38:304–314.
18. Kuroda S, Yamada K, Deguchi T, Hashimoto T, Kyung HM, Takano-Yamamoto T. Root proximity is a major factor for screw failure in orthodontic anchorage. *Am J Orthod Dentofacial Orthop*. 2007;131:S68–S73.
19. Hernández L, Montoto G, Rodríguez M, Galbán L, Martínez V. “Bone map” for a safe placement of miniscrews generated by computed tomography. *Clin Oral Implants Res*. 2008;19:576–581.
20. Park HS. An anatomical study using CT images for the implantation of micro-implants. *Korean J Orthod*. 2002;32:435–441.
21. Liou EJ, Pai BC, Lin JC. Do miniscrews remain stationary under orthodontic forces? *Am J Orthod Dentofacial Orthop*. 2004;126:42–47.
22. Kim SH, Cho JH, Chung KR, Kook YA, Nelson G. Removal torque values of surface-treated mini-implants after loading. *Am J Orthod Dentofacial Orthop*. 2008;134:36–43.
23. Deguchi T, Nasu M, Murakami K, Yabuuchi T, Kamioka H, Yamamoto T. Quantitative evaluation of cortical bone thickness with computed tomographic scanning for orthodontic implants. *Am J Orthod Dentofacial Orthop*. 2006;129:721.e7–721.e12.
24. Byoun NY, Nam EH, Yoon YA, Kim IK. Three-dimensional finite element analysis for stress distribution on the diameter of orthodontic mini-implants and insertion angle to the bone surface. *Korean J Orthod*. 2006;36:178–187.
25. Jabero M, Sarment DP. Advanced surgical guidance technology: a review. *Int J Oral Maxillofac Implants*. 2006;15:135–142.
26. Miyazawa K, Kawaguchi M, Tabuchi M, Goto S. Accurate pre-surgical determination for self-drilling miniscrew implant using surgical guides and cone-beam computed tomography. *Eur J Orthod*. 2010;32:735–740.